Couette Flow in Continuum to Free Molecular Regime

By

Kenichi NANBU*

(February 1, 1983)

Abstract: By use of the direct-simulation method of Nanbu, the Couette flow for wall Mach number 3 is analysed over the whole range of the Knudsen number. Gas is a monatomic one of Maxwell molecules. By comparing the numerical solution obtained from simulation calculations with the approximate six-moment solution of Liu and Lees, the accuracy of the latter is examined in detail. As to the flow velocity and shearing stress, the six-moment solution shows reasonable agreement with the simulation solution. As to the temperature, density, and heat flux, the error of the six-moment solution is not small in all flow regimes except near-continuum one. As to the pressure, it is not uniform in the transition regime, differently from the prediction of the six-moment solution.

1. Introduction

The direct-simulation method of Bird [1] is regarded as a technique for the computer modeling of a real gas flow by some thousands of simulated molecules. It has been developed through reference to the physics of the gas flow rather than through reference to the mathematical description of the flow. Although his method has widely been used, an important question as to whether the simulation solution obtained by use of the method is the exact solution of the Boltzmann equation still remains unanswered. Recently Nanbu [2–4] proposed a new direct-simulation method; all stochastic laws employed in simulation procedure were derived from the Boltzmann equation in a systematic and rigorous manner. (Contrary to the comment of Koura [5], Nanbu's method is quite different from Bird's one in the most important part of the direct-simulation method, i.e., in the stochastic laws for simulating molecular collisions [6]). It was also shown that the use of Nanbu's method reproduces the exact solution discovered by Krook and Wu [7]. The validity of Nanbu's method was further tested by calculating a temporal relaxation of spatially uniform gases initially in large nonequilibrium [8, 9]. At that stage the new direct-simulation method was proved to be a definite solution method of the Boltzmann equation.

Before applying the new direct-simulation method to flow problems, it is also necessary to examine the method in all its technical aspects. The simulation calculations [2, 8, 9] showed in fact that the deviation of the simulation solution from the exact solution of the Boltzmann equation increases with the decrease of N and/or increase of t, where N is the number of the simulated molecules and t is the time. It was found that this fact is closely related to the degree of violation of molecular chaos hypothesis [10]. That is, the correlation of velocity between a molecule and its collision partner increases with t/N. Comparing the error of the simulation solution with the correlation coefficient $\rho(t\,;N)$, it was concluded that the

* Institute of High Speed Mechanics, Tōhoku University.

number N should be chosen in such a way that the condition $\rho(t\,;N)\ll 1$ holds. In making actual simulation calculations, not only the number N but also other simulation parameters such as the sample size, the step size, and the cut-off value of the deflection angle should be chosen in an appropriate manner. A guide for the choice of these parameters was presented in [11].

In the direct-simulation method the flow is always unsteady and a steady flow is obtained as the large time state of the unsteady flow. Two important questions arise in determining the flow properties at the steady state. It appears that if the correlation coefficient $\rho(t\,;N)$ increases with time t, the condition $\rho(t\,;N)\ll 1$ would never hold as $t\to\infty$. The first question is as to whether or not the simulation solution results in a breakdown as $t\to\infty$. This was answered as follows [12]. For usual flows such as the flow past a body or through a channel, the exchange of molecules takes place across the boundaries of a computational flow region; uncorrelated fresh molecules come into the region and correlated molecules go out of the region. In this case $\rho(t\,;N)$ is at most of order N^{-1} no matter how large the time t may be; by use of a large N, $\rho(t\,;N)$ can be made as small as one desires. For confined flows such as the flow in a vessel and the Couette flow considered in this paper, the situation is different, i.e., the molecules never go out of the computational region. In this case the mechanism of keeping $\rho(t\,;N)$ small is the collision of the molecules at a solid wall; if a molecule that strikes the wall is reflected with a refreshed velocity uncorrelated to the one just before a strike, the correlation coefficient $\rho(t\,;N)$ is again of order N^{-1} at any time. A simplest example of such a wall is a diffusely reflecting wall. The second question is the one as to the ergodicity of the simulation solution, i.e., as to whether the time-averaged data agree with the ensemble-averaged data. (Unless the simulation solution were ergodic, the flow properties at the steady state could be determined only through ensemble-averaging, which would take an excessive computing time). Fortunately, the simulation solution is certainly ergodic on condition that the number of molecules and the sampling interval used in obtaining the time-averaged data are so chosen that the correlation coefficient and the correlation function are sufficiently small [13].

The new direct-simulation method of Nanbu was not applied to the flow problems until these preliminary studies were completed. In this paper the Couette flow for wall Mach number 3 is analysed over the whole range of the Knudsen number by use of Nanbu's method. The simulation solution obtained should be regarded as the exact, though numerical, solution of the Boltzmann equation. By using six moment equations, Liu and Lees [14] found an analytical solution of the Couette flow problems over the whole range of the Knudsen number. The accuracy of the approximate solution of Liu and Lees is examined by comparing it with the simulation solution. Also, the solution of the Navier-Stokes equations is obtained by use of slip velocity and temperature jump boundary conditions and compared with the simulation solution.

2. Solution of Six Moment Equations

Liu and Lees [14] employed the six moment equations to find an approximate solution of the problem of the steady Couette flow. The upper wall moves with

velocity $+U/2$ in its own plane at $y=d/2$ and held at temperature T_{I}, while the lower wall at $y=-d/2$ moves parallel to the upper wall with velocity $-U/2$ and is kept at temperature T_{II}. The boundary conditions assumed are completely diffuse reflection and complete thermal accommodation. In this paper our attention is limited to a special case when the temperatures of both walls are equal, i.e., $T_{\mathrm{I}}=T_{\mathrm{II}}=T_w$. The approximate solution of Liu and Lees holds for any value of the Knudsen number; it agrees with the solution of the Navier-Stokes equations at the continuum-flow limit and with the exact solution at the free-molecular limit. Gas is assumed to be a monatomic gas of Maxwell molecules, hence the Chapman-Enskog viscosity and heat conductivity are proportional to temperature.

We rearrange the results of Liu and Lees as follows so that the comparison of these with the simulation solution may become easier. To specify the density level of the gas between the walls, Liu and Lees selected, as a reference density, the density ρ_{II} at $y=-d/2$ of upward streaming molecules. This is somewhat awkward. We re-define the reference density ρ_r as follows. The product of eqs. (40b) and (40c) of [14] shows that the pressure is everywhere constant; we select this constant pressure as a reference pressure p_r, which is considered to be given. The reference density ρ_r is defined by

$$\rho_r=p_r/RT_w, \tag{1}$$

where R is the gas constant per unit mass. The ratio of p_r to $p_{\mathrm{II}}(=\rho_{\mathrm{II}}RT_w)$ is, from the product of eqs. (40b) and (40c) of [14]

$$\frac{p_r}{p_{\mathrm{II}}}=\frac{\alpha_2}{2}\left(1+\frac{1}{3}\gamma M^2\frac{\alpha_1^2}{\alpha_2^2}\right), \tag{2}$$

where γ $(=5/3)$ is the ratio of specific heats, $M[=U/(\gamma RT_w)^{1/2}]$ is the wall Mach number, and α_2 is defined by

$$\alpha_2=1+\left[1-\frac{s}{4}\alpha_1(1+\alpha_1)\right]^{1/2}, \tag{3}$$

with $s=\gamma M^2$. The constant α_1 is the solution of the following algebraic equation [14]

$$(\lambda_1\lambda_2-\lambda_3)(2-\alpha_2)^3+\lambda_2(2-\alpha_2)+\frac{4}{(2\pi\gamma)^{1/2}}\left(\frac{R_e}{M}\right)\frac{\alpha_1}{\alpha_2}=0, \tag{4}$$

where

$$\lambda_1=\frac{21+s(\alpha_1/\alpha_2)^2+(32/s)(\alpha_2/\alpha_1)^2}{3(s\alpha_1^2+5\alpha_2^2)}, \tag{5a}$$

$$\lambda_2=\alpha_2\left(\frac{4}{s}\frac{\alpha_2}{\alpha_1}-\frac{\alpha_1}{\alpha_2}\right), \tag{5b}$$

$$\lambda_3=\frac{1}{3}\left(\alpha_2\lambda_1+\frac{1}{\alpha_2}\right)\left(\frac{4}{s}\frac{\alpha_2}{\alpha_1}-\frac{\alpha_1}{\alpha_2}\right). \tag{5c}$$

The ratio R_e/M in eq. (4) is rewritten as [14]

$$\frac{R_e}{M}=\left(\frac{\pi\gamma}{2}\right)^{1/2}\frac{d}{\lambda_{II}}, \tag{6}$$

where λ_{II} (the mean free path at density ρ_{II} and temperature T_w) is defined by

$$\lambda_{II}=\frac{\mu_w}{\rho_{II}}\left(\frac{\pi}{2RT_w}\right)^{1/2}. \tag{7}$$

Here μ_w is the Chapman-Enskog viscosity at temperature T_w. Since R_e/M depends on ρ_{II}, it is not a convenient parameter. In place of R_e/M we introduce the Knudsen number defined by

$$K_n=\frac{\lambda_r}{d}, \tag{8}$$

where

$$\lambda_r=\frac{\mu_w}{\rho_r}\left(\frac{\pi}{2RT_w}\right)^{1/2}. \tag{9}$$

The relation between R_e/M and K_n can be obtained from eqs. (6) to (9):

$$\frac{R_e}{M}=\left(\frac{\pi\gamma}{2}\right)^{1/2}\left(\frac{p_r}{p_{II}}\right)^{-1}K_n^{-1}, \tag{10}$$

where $p_r=\rho_r RT_w$ and $p_{II}=\rho_{II}RT_w$ are used. By use of eqs. (2) and (10), eq. (4) takes the form

$$(\lambda_1\lambda_2-\lambda_3)(2-\alpha_2)^3+\lambda_2(2-\alpha_2)+\frac{4\alpha_1}{\alpha_2^2}\left(1+\frac{s}{3}\frac{\alpha_1^2}{\alpha_2^2}\right)^{-1}K_n^{-1}=0. \tag{11}$$

Once M and K_n are given, this equation determines α_1, which is $-1<\alpha_1<0$. Then the constants α_2 and λ's are readily determined from eqs. (3) and (5).

The flow velocity u, the temperature T, the density ρ, and the pressure p are given by

$$\frac{u}{U}=-\left(\frac{2}{s}\frac{\alpha_2}{\alpha_1}+\frac{1}{2}\frac{\alpha_1}{\alpha_2}\right)F, \tag{12}$$

$$\frac{T}{T_w}=\frac{1}{4}\left(1+\frac{s}{3}\frac{\alpha_1^2}{\alpha_2^2}\right)(\alpha_2^2G^2-F^2), \tag{13}$$

$$\frac{\rho}{\rho_r}=\left(\frac{T}{T_w}\right)^{-1}, \tag{14}$$

$$\frac{p}{p_r}=1. \tag{15}$$

Here, F is a function of $\tilde{y}\,(=y/d)$ and satisfies the cubic equation

$$F^3-3AF+2B=0, \tag{16}$$

where

$$A=\frac{\lambda_2}{3\lambda_3}\alpha_5,$$

$$B=\frac{4\alpha_1}{\lambda_3\alpha_2^2}\left(1+\frac{s}{3}\frac{\alpha_1^2}{\alpha_2^2}\right)^{-1}K_n^{-1}\tilde{y},$$

with

$$\alpha_5=1+\lambda_1(2-\alpha_2)^2.$$

The solution of eq. (16) is [15]

$$F(\tilde{y})=2A^{1/2}\sin\left[\frac{1}{3}\left(\theta-\frac{\pi}{2}\right)\right], \tag{17}$$

where

$$\theta=\cos^{-1}\left(-\frac{B}{A^{3/2}}\right), \qquad (0<\theta<\pi).$$

The function $G(\tilde{y})$ is given by

$$G=(\alpha_5-\lambda_1F^2)^{1/2}. \tag{18}$$

Note that u is an odd and T is an even function of $\tilde{y}$. The shearing stress τ_{xy} and heat flux q_y are, in nondimensional forms

$$\tilde{\tau}_{xy}=-\left(\frac{s}{2\pi}\right)^{1/2}\left(1+\frac{s}{3}\frac{\alpha_1^2}{\alpha_2^2}\right)^{-1}\frac{\alpha_1}{\alpha_2}, \tag{19}$$

$$\tilde{q}_y=\frac{1}{\pi^{1/2}}\left(1+\frac{s}{3}\frac{\alpha_1^2}{\alpha_2^2}\right)^{-1}\left(1+\frac{s}{4}\frac{\alpha_1^2}{\alpha_2^2}\right)F(\tilde{y}), \tag{20a}$$

$$(\tilde{q}_y)_w=\frac{\alpha_2-2}{\pi^{1/2}}\left(1+\frac{s}{3}\frac{\alpha_1^2}{\alpha_2^2}\right)^{-1}\left(1+\frac{s}{4}\frac{\alpha_1^2}{\alpha_2^2}\right), \tag{20b}$$

where $\tilde{\tau}_{xy}=\tau_{xy}/[\rho_r(2RT_w)]$, $\tilde{q}_y=q_y/[\rho_r(2RT_w)^{3/2}]$, and $(\tilde{q}_y)_w$ denotes the heat flux to the upper wall. (The heat flux to the lower wall is $-(\tilde{q}_y)_w$.) Note that the shearing stress does not depend on $\tilde{y}$. Table 1 gives α_1, $\tilde{\tau}_{xy}$, $(\tilde{q}_y)_w$ for $M=3$ and

Table 1. Values of α_1, $\tilde{\tau}_{xy}$, $(\tilde{q}_y)_w$ for $M=3$ (Liu-Lees solution)

K_n	α_1	$\tilde{\tau}_{xy}$	$(\tilde{q}_y)_w$
0.03473	−0.09690	0.06886	0.08580
0.06417	−0.1776	0.1186	0.1366
0.1183	−0.3017	0.1841	0.1870
0.2628	−0.4944	0.2631	0.2114
0.4906	−0.6279	0.3030	0.1950
0.9407	−0.7358	0.3263	0.1627
2.281	−0.8368	0.3403	0.1162
4.515	−0.8882	0.3441	0.08573
9.001	−0.9242	0.3454	0.06132

various values of K_n.

Consider the continuum and free-molecular limit. In the limiting case of $K_n \to 0$, we have

$$\frac{u}{U} = -\frac{4}{s} F_0, \tag{21}$$

$$\frac{T}{T_w} = \alpha_5 - \frac{32}{15s} F_0^2, \tag{22}$$

where

$$F_0(\tilde{y}) = 2A_0^{1/2} \sin\left[\frac{1}{3}\left(\theta_0 - \frac{\pi}{2}\right)\right],$$

with

$$\theta_0 = \cos^{-1}\left(-\frac{B_0}{A_0^{3/2}}\right), \qquad (0 < \theta_0 < \pi)$$

$$A_0 = \frac{15}{32} s\left(1 + \frac{1}{30} s\right),$$

$$B_0 = -\frac{45}{256} s^2\left(1 + \frac{1}{45} s\right)\tilde{y}.$$

The shearing stress and heat flux take the forms

$$\tilde{\tau}_{xy} = \left(\frac{s}{2\pi}\right)^{1/2}\left(1 + \frac{1}{45} s\right) K_n, \tag{23}$$

$$(\tilde{q}_y)_w = \frac{s}{4\pi^{1/2}}\left(1 + \frac{1}{45} s\right) K_n. \tag{24}$$

Although $\tilde{\tau}_{xy}$ and $(\tilde{q}_y)_w$ are $O(K_n)$, these correspond to eqs. (21) and (22) which are O(1). In the other limiting case of $K_n \to \infty$, we have

$$\frac{u}{U} = \frac{6(16+s)}{(16-s)(12+s)} K_n^{-1} \tilde{y} \to 0, \tag{25}$$

$$\frac{T}{T_w} = 1 + \frac{1}{12} s, \tag{26}$$

$$\tilde{\tau}_{xy} = \left(\frac{s}{8\pi}\right)^{1/2}\left(1 + \frac{1}{12} s\right)^{-1}, \tag{27}$$

$$(\tilde{q}_y)_w = \frac{9s(16+s)}{\pi^{1/2}(12+s)^2(16-s)} K_n^{-1} \to 0. \tag{28}$$

If K_n is large but finite in eq. (25), u must be positive for $\tilde{y} > 0$, so that $16 - s > 0$ or $M < 3.098$ must hold, i.e., there is a 'critical' Mach number in the solution of Liu and Lees [14].

Equations (21) to (24) agree with the results obtained by solving the Navier-

Stokes equations by use of boundary conditions of no slip velocity and no temperature jump. On the other hand, eqs. (25) to (28) are exact because the two-stream Maxwellian distribution assumed by Liu and Lees becomes exact at the free-molecular limit. That is, the solution of Liu and Lees is exact for both limiting cases of $K_n=0$ and ∞.

3. Solution of the Navier-Stokes Equations

The Navier-Stokes equations, together with slip velocity and temperature jump boundary conditions, are considered to be adequate for the Knudsen number of the order of 0.01 to 0.1 [16]. The solution of the Navier-Stokes equations is given here to make a comparison with the simulation solution. The Navier-Stokes equations are [17]

$$\frac{dp}{dy}=0, \tag{29}$$

$$\frac{d}{dy}\left(\mu\frac{du}{dy}\right)=0, \tag{30}$$

$$\frac{d}{dy}\left[\mu\left(\frac{3c_p}{2}\frac{dT}{dy}+u\frac{du}{dy}\right)\right]=0, \tag{31}$$

where μ is the coefficient of viscosity and c_p $(=5R/2)$ is the specific heat at constant pressure. The boundary conditions are

$$u=\frac{U^*}{2} \quad \text{and} \quad T=T^* \quad \text{at} \quad y=+\frac{d}{2}, \tag{32a}$$

$$u=-\frac{U^*}{2} \quad \text{and} \quad T=T^* \quad \text{at} \quad y=-\frac{d}{2}, \tag{32b}$$

where

$$\frac{U^*}{2}=\frac{U}{2}-u_s, \tag{33a}$$

$$T^*=T_w+T_j. \tag{33b}$$

The slip velocity u_s for completely diffuse reflection and the temperature jump T_j for complete thermal accommodation take the forms [18]

$$u_s=\lambda\frac{du}{dy}, \tag{34a}$$

$$T_j=\frac{15}{8}\left|\lambda\frac{dT}{dy}\right|. \tag{34b}$$

The right-hand sides of eqs. (34) should be evaluated at $y=+d/2$ or $-d/2$. The mean free path λ should be evaluated at the gas temperature (and the gas density) at the wall, and not the wall temperature. Note that the symmetry of the boundary condi-

tions implies that u is an odd and T is an even function of y.

Equation (29) shows that the pressure is everywhere constant as it is for the Liu-Lees solution. Let the pressure be p_r as before. The solution of eqs. (30) and (31) can be obtained after the manner in [17]. (Regard the wall velocities as $\pm U^*/2$ and the wall temperatures as T^*, and obtain the solution by use of no slip and jump boundary conditions.) The flow velocity u is

$$\tilde{y}=\left(1+\frac{2}{3}\alpha^*\right)^{-1}\left[(1+\alpha^*)\frac{u}{U^*}-\frac{4\alpha^*}{3}\left(\frac{u}{U^*}\right)^3\right], \tag{35a}$$

where

$$\alpha^*=\frac{U^{*2}}{12c_pT^*}.$$

The solution of this cubic equation is

$$\frac{u}{U^*}=A_1^{1/2}\sin\left[\frac{1}{3}\left(\theta_1-\frac{\pi}{2}\right)\right], \tag{35b}$$

where

$$\theta_1=\cos^{-1}\left(-\frac{B_1}{A_1^{3/2}}\right), \qquad (0<\theta_1<\pi)$$
$$A_1=1+\alpha^{*-1},$$
$$B_1=\left(1+\frac{3}{2\alpha^*}\right)(2\tilde{y}).$$

The temperature is

$$\frac{T}{T^*}=1+\alpha^*\left[1-\left(\frac{2u}{U^*}\right)^2\right]. \tag{36}$$

The quantities U^* and T^* can be determined from eqs. (34) as follows. Define the mean free path λ^* by

$$\lambda^*=\frac{\mu^*}{\rho^*}\left(\frac{\pi}{2RT^*}\right)^{1/2}, \tag{37}$$

where $\rho^*=p_r/RT^*$ and μ^* is the coefficient of viscosity at temperature T^*. The mean free path λ in eqs. (34) must be replaced by λ^*. From eqs. (9) and (37) we have

$$\frac{\lambda^*}{\lambda_r}=\left(\frac{T^*}{T_w}\right)^{3/2}. \tag{38}$$

Using eqs. (34), (35a), and (36), we have from eqs. (33)

$$\frac{U^*}{U}=1-2\left(1+\frac{2}{3}\alpha^*\right)\left(\frac{U^*}{U}\right)\left(\frac{\lambda^*}{\lambda_r}\right)K_n, \tag{39a}$$

$$\frac{T^*}{T_w}=1+\frac{15}{2}\alpha^*\left(1+\frac{2}{3}\alpha^*\right)\left(\frac{T^*}{T_w}\right)\left(\frac{\lambda^*}{\lambda_r}\right)K_n, \tag{39b}$$

where

$$\alpha^*=\alpha\left(\frac{U^*}{U}\right)^2\left(\frac{T^*}{T_w}\right)^{-1}, \tag{40}$$

with

$$\alpha=\frac{U^2}{12c_pT_w}=\frac{1}{30}\gamma M^2.$$

Substitution of eqs. (38) and (40) into (39) shows that eqs. (39) are a set of coupled equations for U^*/U and T^*/T_w. Neglecting the terms of order K_n^2, K_n^3, $\cdots$, we obtain

$$\frac{U^*}{U}=1-2\left(1+\frac{2}{3}\alpha\right)K_n, \tag{41a}$$

$$\frac{T^*}{T_w}=1+\frac{15}{2}\alpha\left(1+\frac{2}{3}\alpha\right)K_n. \tag{41b}$$

Once M and K_n are given, then u/U and T/T_w are determined from eqs. (35b), (36), and (41) by use of $u/U=(u/U^*)(U^*/U)$ and $T/T_w=(T/T^*)(T^*/T_w)$. It can be shown that in the limiting case of $K_n\to 0$, the Liu-Lees solution given by eqs. (21) to (24) agrees with the Navier-Stokes solution.

4. Solution from Simulation Calculations

4.1 Outline of Simulation Procedure

In the direct-simulation method the flow is always unsteady and a steady flow is obtained as the large time state of the unsteady flow. Before starting the simulation calculation initial conditions for simulated molecules must be specified. Here it is assumed that gas is initially in equilibrium at temperature T_0 and density ρ_0; T_0 and ρ_0 are everywhere constant. The temperature T_0 is chosen to be equal to the wall temperature T_w. Two flow parameters must also be given before starting the calculation. One is the wall Mach number M. Of course, one can give M any value in advance. The other is the Knudsen number. However, one cannot know the value of K_n defined by eq. (8) until the steady flow is established. A related parameter to which one can give a value at time $t=0$ is the Knudsen number K_{n0} defined by

$$K_{n0}=\frac{\lambda_0}{d}, \tag{42}$$

where λ_0 is the mean free path at $t=0$, i.e.

$$\lambda_0=\frac{\mu_w}{\rho_0}\left(\frac{\pi}{2RT_w}\right)^{1/2}. \tag{43}$$

As will be seen later, the Knudsen number K_n is a function of K_{n0} and M.

The flow from $y=-d/2$ to $d/2$ is divided into J cells. Since ρ_0 is constant, the number N_0 of the simulated molecules in each cell is equal at $t=0$. These molecules are distributed uniformly in each cell. The initial velocity of each molecule is sampled from the equilibrium distribution at temperature T_w. Once the positions and velocities of the simulated molecules are given at $t=0$, these at later time-points $t=\Delta t$, 2Δ, . . . can be determined step by step [8]. The principle of uncoupling makes it possible to treat molecular displacement and intermolecular collision separately. First, the molecule is moved freely over Δt. Some molecules are reflected at the wall surface during this motion. Next, the collision is calculated. Let $N_{j,k}$ be the number of molecules in cell j at time-point $k\Delta t$. The collision probability $P_{j,k}$ of a molecule in cell j over one time-step from $(k-1)\ \Delta t$ to $k\Delta t$ is given by

$$P_{j,k}=K\left(\frac{N_{j,k}-1}{N_0}\right)\Delta\hat{t}, \tag{44}$$

where $\Delta\hat{t}$ is the time step measured in units of $\lambda_0/(2RT_w)^{1/2}$, $K=\pi^{1/2}\beta_0^2/[3A_2(4)]$, and $A_2(4)=0.4362$. The value of K is 7.743 for $\beta_0=2.391$, which is corresponding to the cut-off angle of 2° [8].

A set of velocities of $N_{j,k}$ molecules in cell j plays the role of the velocity-distribution function, i.e., it determines the flow properties at the center of cell j at time-point $k\Delta t$. The gas density $\rho_{j,k}$ and the flow velocity $\bar{c}_{j,k}$ are determined from

$$\frac{\rho_{j,k}}{\rho_0}=\frac{N_{j,k}}{N_0}, \tag{45}$$

$$\bar{c}_{j,k}=\frac{1}{N_{j,k}}\sum_i c_{i,k}, \tag{46}$$

where $c_{i,k}$ is the velocity of the ith molecule and the summation is over all molecules in cell j. Similarly, the temperature $T_{j,k}$ is determined from

$$T_{j,k}=\frac{1}{3R}\left(\frac{N_{j,k}}{N_{j,k}-1}\right)\left(\frac{1}{N_{j,k}}\sum_i c_{i,k}^2-\bar{c}_{j,k}^2\right), \tag{47}$$

where $\bar{c}_{j,k}^2=(\bar{c}_x)_{j,k}^2+(\bar{c}_y)_{j,k}^2+(\bar{c}_z)_{j,k}^2$. When the flow is in the steady state, $(\bar{c}_y)_{j,k}$ and $(\bar{c}_z)_{j,k}$ vanish except for statistical fluctuations. Since the fluctuations are never null for a finite $N_{j,k}$, however, one must not set $(\bar{c}_y)_{j,k}=(\bar{c}_z)_{j,k}=0$. The shearing stress τ_{xy} and heat flux $(q_y)_w$ are based on the sampled flux of molecular number, momentum, and energy incident on and reflected from the wall. Introduce the nondimensional variables by dividing velocity by $(2RT_w)^{1/2}$, length by λ_0, and time by $\lambda_0/(2RT_w)^{1/2}$, and denote such variables by a caret placed over the symbol. Then, τ_{xy} and $(q_y)_w$ are given by

$$\frac{\tau_{xy}}{\rho_0(2RT_w)}=\left[\frac{\hat{U}}{2}-(\hat{\bar{c}}_x)_i\right]\frac{N_T\Delta\hat{y}}{N_0(\hat{t}_2-\hat{t}_1)}, \tag{48}$$

$$\frac{q_y}{\rho_0(2RT_w)^{3/2}}=\frac{1}{2}\left[\frac{\hat{U}}{2}+(\hat{\bar{c}}_x)_i\right]\frac{\tau_{xy}}{\rho_0(2RT_w)}, \tag{49}$$

where $\Delta\hat{y}$ is the cell height, N_T is the total number of the molecules that are incident on the unit area of the wall from time $\hat{t}_1$ to $\hat{t}_2$, and $(\hat{\bar{c}}_x)_i$ is the x-component of the mean velocity of such molecules.

4.2 Results of Simulation Calculations

4.2.1 Preliminaries

Although a full unsteady flow is calculated, our concern is in the ultimate steady flow. The flow properties in the steady state can be determined through the time-averaging of the simulation data of eqs. (45) to (47). Before doing so, however, the time at which the flow practically becomes steady must be determined. This can be done through the ensemble-averaging. Preliminary calculations are made for $K_{n0}=0.05$ by use of $J=20$ and $\Delta\hat{t}=0.01$, where J is the number of cells and $\Delta\hat{t}$ is the time step. The value of $\Delta\hat{t}$ is so chosen that $P_{j,k}$ of eq. (44) satisfies the condition $P_{j,k}\ll 1$ [2]. The choice of the number N_0 of molecules per cell is of crucial importance; if N_0 is too small, the simulation data include the error ascribable to the correlation of velocity between a molecule and its collision partner [10, 12]. The calculations are made for $N_0=50$, 100, and 200. The time $\hat{t}$ is advanced up to 300. All calculations from $\hat{t}=0$ to 300 are repeated M_E times by using M_E independent initial conditions for molecules. The result forms a set of M_E members of an ensemble. The number M_E is so chosen that the sample size N_0M_E takes a fixed value 1000 for any N_0. Comparing the ensemble-averaged data of the flow velocity $(\bar{c}_x)_{j,k}$ at $\hat{t}=k\Delta\hat{t}=10$, 20, 30, $\cdots$, we have seen that the flow is practically steady for $\hat{t}\geq 50$ for all three values of N_0. In order to exclude any unsteadiness we have concluded for safety that the flow is steady for $\hat{t}\geq 200$. Clearly, this fact for $K_{n0}=0.05$ is true also for $K_{n0}>0.05$. The reason is that when the initial mean free path λ_0 is fixed, the frequency of molecular collision with the wall increases with decreasing the height d (i.e., increasing K_{n0}), which results in decreasing the time taken for the flow to settle down into the steady state.

Whether N_0 is large or small makes a subtle difference in the simulation data; it is covered with the statistical fluctuations if the sample size is of order 1000. On the other hand, a typical calculation of the ensemble-averaged data of the sample size 1000 takes about 4 hours on the high speed digital computer (ACOS 1000 of the Computing Center of Tōhoku University), so that it is impracticable to increase the sample size by a large margin. In order to examine the effect of N_0 we are obliged to resort to the time-averaged data, the sample size of which can be made much larger. (A typical calculation of the time-averaged data of the sample size 50000 takes about 3 hours.) The time-averaged data are obtained by summing a sequence of the of the flow properties at $\hat{t}=200+(l-1)\hat{h}$ $(l=1, 2, \cdots, L)$. The sampling interval $\hat{h}$ must be greater than 1 [13]. The greater the interval, the better the data. The preliminary culculations are made for $\hat{h}=5$. The sample size N_0L is fixed at 50000 for any N_0, so that L is, e.g., 250 for $N_0=200$. Let ρ, u, and T be, in turn, the time-averaged data of $\rho_{j,k}$, $(\bar{c}_x)_{j,k}$, and $T_{j,k}$. To see

the effect of N_0, the data ρ, u, T are obtained for $N_0=50$, 100, 200. We have seen that the effect of N_0 is most remarkable in T; the temperature for $N_0=100$ agrees with that for $N_0=200$, whereas the temperature for $N_0=50$ is rather lower than that for $N_0=200$. Since the flow properties must not depend on the number N_0, one should use N_0 greater than 100.

4.2.2 Results

Full simulation calculations are made for a fixed Mach number $M=3$, which is lower than the critical Mach number 3.098 of the Liu-Lees solution. The Knudsen number K_{n0} is changed between 0.05 and 20. The simulation parameters used are as follows.

time step: $\Delta\hat{t}=0.01$,
cell number: $J=20$ for $K_{n0}\leq 2$ and $J=10$ for $K_{n0}>2$,
initial molecular number per cell: $N_0=200$,
sample size: $N_0L=50000$,
sampling interval: $\hat{h}=3$,
starting time of sampling: $\hat{t}_1=200$.

The choice of these is based on the preliminary calculations. The cell number J is reduced to 10 for $K_{n0}>2$. The reason is that as eqs. (25) and (26) show, the variation of the flow properties between the two walls is small for large Knudsen number. The sampling interval $\hat{h}$ is reduced to 3 to save the computing time.

We are concerned only with the flow in the steady state. The Knudsen number K_n $(=\lambda_r/d)$ defined by eq. (8) is preferred to K_{n0} in describing the steady flow. The reference density in eq. (9) is defined by $\rho_r=p_r/RT_w$, where p_r is the pressure for the steady flow. Both the Liu-Lees solution and the Navier-Stokes solution show that the pressure p is everywhere constant. This constant pressure is chosen as a reference pressure p_r. The simulation solution shows, however, that this is true only for $K_n\ll 1$ or $K_n\gg 1$. In the transition regime the pressure p shows a weak dependence on y. Therefore, p_r is defined here as the mean pressure, i.e.

$$p_r=\frac{1}{J}\sum_{j=1}^{J}p_j,$$

where p_j is the pressure at the center of cell j. The relation between K_n and K_{n0} is, from eqs. (8), (9), (42), and (43)

$$K_n=\left(\frac{p_r}{p_0}\right)^{-1}K_{n0}, \tag{50}$$

where $p_0=\rho_0RT_w$. The ratio p_r/p_0 can be determined as follows. The time-averages of eqs. (45) and (47) give ρ/ρ_0 and T/T_w. The product of ρ/ρ_0 and T/T_w is equal to p/p_0, the mean value of which is p_r/p_0. Table 2 gives p_r/p_0 and K_n for various values of K_{n0}. (The wall Mach number is 3.) Once ρ_r/p_0 is determined, ρ/ρ_r and p/p_r are given by

$$\frac{\rho}{\rho_r}=\left(\frac{p_r}{p_0}\right)^{-1}\left(\frac{\rho}{\rho_0}\right), \tag{51}$$

$$\frac{p}{p_r}=\left(\frac{p_r}{p_0}\right)^{-1}\left(\frac{p}{p_0}\right). \tag{52}$$

The shearing stress $\tilde{\tau}_{xy}$ and heat flux $(\tilde{q}_y)_w$ are

$$\tilde{\tau}_{xy}=\left(\frac{p_r}{p_0}\right)^{-1}\left[\frac{\tau_{xy}}{\rho_0(2RT_w)}\right], \tag{53}$$

$$(\tilde{q}_y)_w=\left(\frac{p_r}{p_0}\right)^{-1}\left[\frac{(q_y)_w}{\rho_0(2RT_w)^{3/2}}\right]. \tag{54}$$

The bracketed expressions in eqs. (53) and (54) are given by eqs. (48) and (49).

The flow properties u/U, T/T_w, ρ/ρ_r, p/p_r, and wall properties $\tilde{\tau}_{xy}$, $(\tilde{q}_y)_w$ thus determined are now compared with the Liu-Lees solution given by eqs. (12), (13), (14), (15), (19), (20b) and the Navier-Stokes solution calculated from eqs. (35b), (36). Figure 1 shows the flow velocity u/U. The solid curves represent the Liu-Lees solution and the symbols represent the simulation solution. The results for $K_n \geq 0.0642$ are shifted to the right; the vertical lines represent $u/U=0$. The Navier-Stokes solution is not shown in Fig. 1. However, comparison of the Navier-Stokes

Table 2. Values of p_r/p_0, K_n, $\tilde{\tau}_{xy}$, $(\tilde{q}_y)_w$ for $M=3$ (simulation solution)

K_{n0}	p_r/p_0	K_n	$\tilde{\tau}_{xy}$	$(\tilde{q}_y)_w$
0.05	1.440	0.03473	0.07370	0.09047
0.1	1.558	0.06417	0.1156	0.1305
0.2	1.690	0.1183	0.1704	0.1669
0.5	1.902	0.2628	0.2373	0.1728
1	2.038	0.4906	0.2749	0.1471
2	2.126	0.9407	0.3030	0.1111
5	2.192	2.281	0.3252	0.06549
10	2.215	4.515	0.3351	0.04033
20	2.222	9·001	0.3412	0.02365

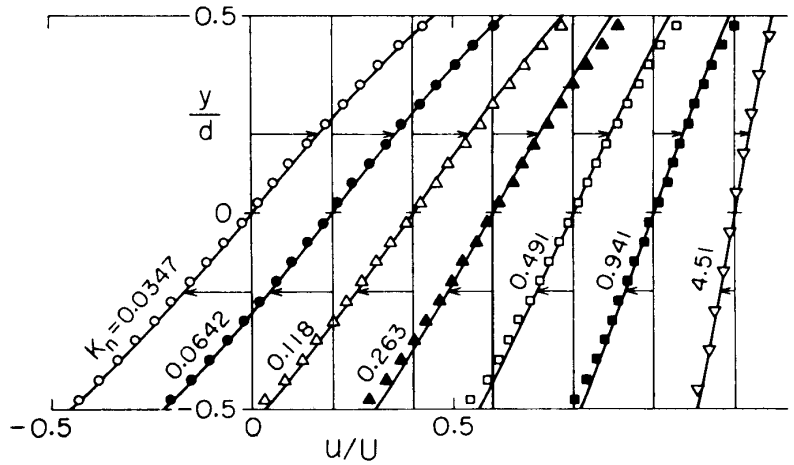

Fig. 1. Velocity profiles for $M=3$. The symbols represent the simulation solution and the solid curves represent the six-moment solution.

and Liu-Lees solution has shown: the Navier-Stokes solution for $K_n=0.0347$ is indistinguishable from the corresponding Liu-Lees solution; a slight difference appears between the two at $K_n=0.0642$; the difference is of an appreciable magnitude at $K_n=0.118$. The magnitude of the slip velocity given by the Navier-Stokes solution amounts to 9% of the wall velocity $U/2$ at $K_n=0.0347$, 17% at $K_n=0.0642$, and 32% at $K_n=0.118$. Since an upper limit of the slip correction for the Navier-Stokes solution may be about 10%, only the Navier-Stokes solution for the lowest K_n, which agrees with the Liu-Lees solution, is considered to be accurate. For this reason we hereafter dispense with the comparison of the simulation solution and the Navier-Stokes solution. The simulation solution, though numerical, is exact, so that we can now examine the accuracy of the approximate solution of Liu and Lees. It is seen from Fig. 1 that the Liu-Lees solution generally agrees with the simulation solution for any K_n. In particular, the agreement is very good for both limits of the smallest and largest K_n, which is consistent with the fact that the Liu-Lees solution is exact at $K_n=0$ and ∞. In the transition regime of $0.118 \leq K_n \leq 0.941$, the Liu-Lees solution shows a deviation from the simulation solution near the walls; the slip velocity of the Liu-Lees solution is somewhat greater than that of the simulation solution.

Figure 2 shows the temperature T/T_w. It is seen that the Liu-Lees solution is accurate at $K_n=0.0347$. However, the error of the Liu-Lees solution is large in the transition regime. Figure 3 shows the density ρ/ρ_r. Again the Liu-Lees solution is accurate at $K_n=0.0347$. The Liu-Lees solutions for all other K_n's are qualitatively correct. Figure 4 shows the pressure distributions. The results for $K_n \geq 0.0642$ are shifted to the right; the vertical lines represent $p/p_r=1$. The Liu-Lees solution predicts that the pressure is everywhere constant for any K_n. It is seen from Fig. 4 that this is true only for the smallest and largest K_n. In the transition regime the pressure lowers near the walls. Figure 5 shows the nondimensional shearing stress $\tilde{\tau}_{xy}$ as a function of K_n. The Liu-Lees solution shows reasonable agreement with the

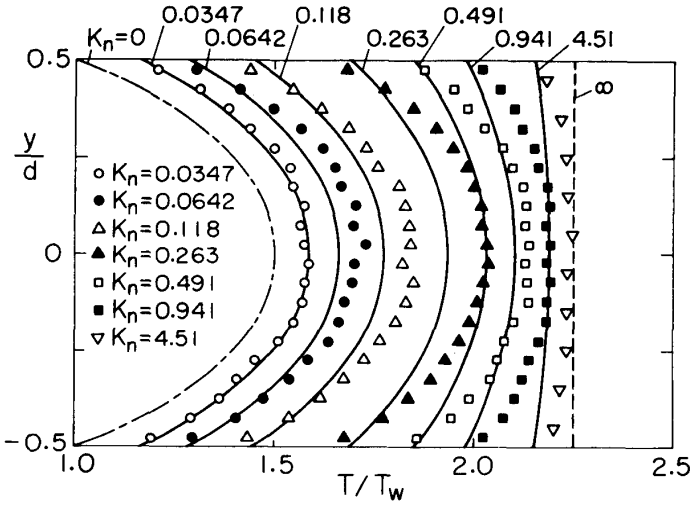

Fig. 2. Temperature profiles for $M=3$. The symbols represent the simulation solution and the solid curves represent the six-moment solution.

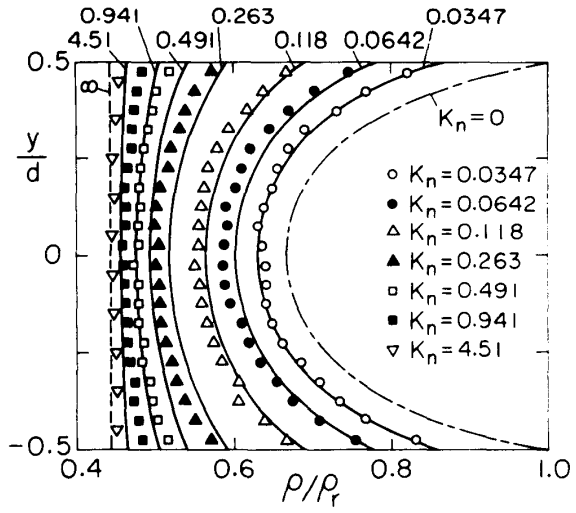

Fig. 3. Density profiles for $M=3$. The symbols represent the simulation solution and the solid curves represent the six-moment solution.

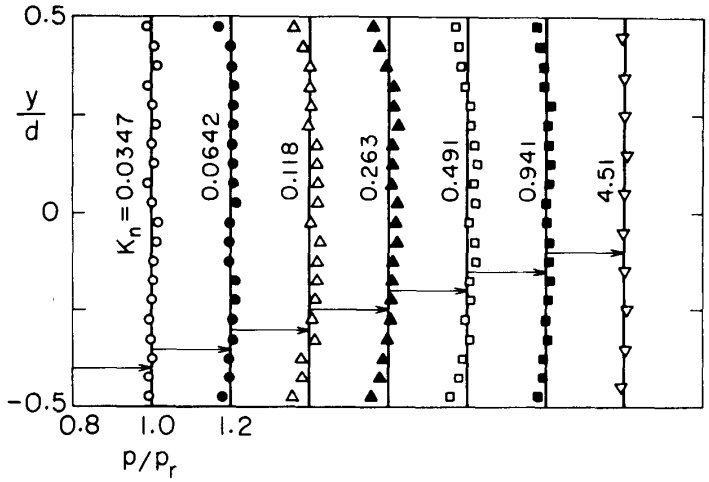

Fig. 4. Pressure distributions for $M=3$. The symbols represent the simulation solution and the solid lines represent the six-moment solution.

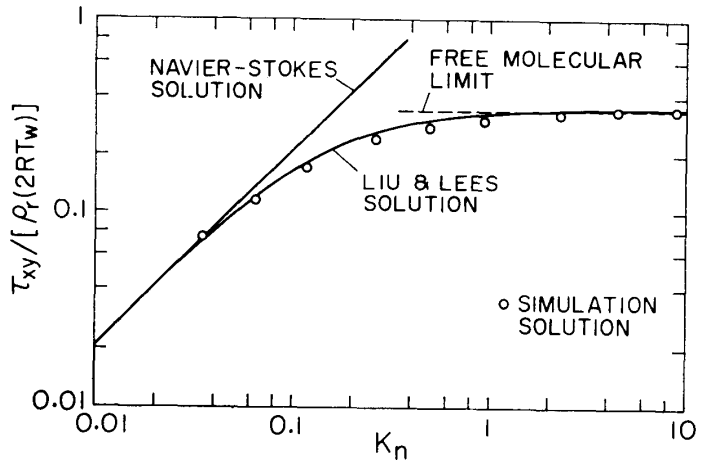

Fig. 5. Shearing stress for $M=3$.

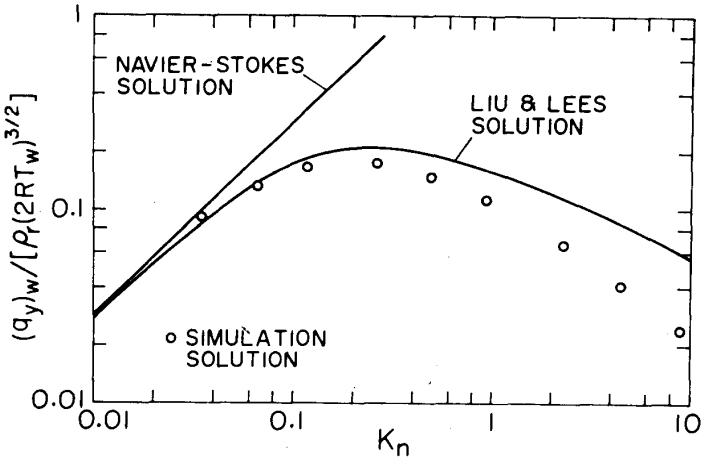

Fig. 6. Heat flux for $M=3$.

simulation solution, which is consistent with the agreement of the velocity profiles given by the two solutions. The continuum-flow limit is given by eq. (23), which is represented as the Navier-Stokes solution in Fig. 5. Note that the Liu-Lees solution slightly overshoots the free molecular limit given by eq. (27) before settling down into the limit. Figure 6 shows the nondimensional heat flux $(\tilde{q}_y)_w$. It takes the maximum near $K_n=0.2$. Equation (24) is represented as the Navier-Stokes solution. As K_n increases, the Liu-Lees solution deviates from the simulation solution. Table 2 gives the values of $\tilde{\tau}_{xy}$ and $(\tilde{q}_y)_w$ determined from the simulation calculation.

5. Conclusions

By use of the direct-simulation method of Nanbu, the steady Couette flow for wall Mach number 3 is analysed over the whole range of the Knudsen number. The obtained solution is the exact numerical solution of the Boltzmann equation, although it includes small statistical fluctuaations. The accuracy of the approximate solution of Liu and Lees is examined by comparing it with the simulation solution. The results are summarized as follows.

(1) The velocity profile of the Liu-Lees solution generally agrees with that of the simulation solution for any Knudsen number. Strictly speaking, however, the slip velocity of the Liu-Lees solution is somewhat greater than that of the simulation solution in the transition flow regime.

(2) The temperature profile of the Liu-Lees solution is accurate in the near-continuum flow regime. In the transition flow regime, however, the difference of temperature profile between the Liu-Lees and the simulation solution is fairly large.

(3) The density profile of the Liu-Lees solution is also accurate in the near-continuum flow regime. In all other flow regimes, however, it is only qualitatively correct.

(4) The prediction of the Liu-Lees solution that the pressure is everywhere constant is correct only for small or large Knudsen number. In the transition flow regime, the pressure lowers near the walls.

(5) The shearing stress of the Liu-Lees solution generally shows reasonable agreement with the simulation solution in all flow regimes, although the former gives a slight overestimation in the transition flow regime.

(6) The heat flux of the Liu-Lees solution agrees with that of the simulation solution in the near-continuum flow regime. Beyond the regime, however, the error of the Liu-Lees solution increases with the Knudsen number.

References

[1] G. A. Bird: Molecular Gas Dynamics, Oxford Univ. Press, London, 1976, pp. 118–132.

[2] K. Nanbu: Direct Simulation Scheme Derived from the Boltzmann Equation. I. Monocomponent Gases, J. Phys. Soc. Japan, Vol 49 (1980), pp. 2042–2049.

[3] K. Nanbu: Direct Simulation Scheme Derived from the Boltzmann Equation. II. Multicomponent Gas Mixtures, J. Phys. Soc. Japan, Vol. 49 (1980), pp. 2050–2054.

[4] K. Nanbu: Direct Simulation Scheme Derived from the Boltzmann Equation. III. Rough Sphere Gases, J. Phys. Soc. Japan, Vol. 49 (1980), pp. 2055–2058.

[5] K. Koura: Comment on "Direct Simulation Scheme Derived from the Boltzmann Equation. I. Monocomponent Gases", J. Phys. Soc. Japan, Vol. 50 (1981), pp. 3829–3830.

[6] K. Nanbu: Reply to a Comment by Koura on "Direct Simulation Scheme Derived from the Boltzmann Equation. I. Monocomponent Gases", J. Phys. Soc. Japan, Vol. 50 (1981), pp. 3831–3832.

[7] M. Krook and T. T. Wu: Exact Solutions of the Boltzmann Equation, Phys. Fluids, Vol. 20 (1977), pp. 1589–1595.

[8] K. Nanbu and Y. Watanabe: Relaxation Rates of Inverse-Power and Rigid-Sphere Molecules, Rep. Inst. High Speed Mech., Tōhoku Univ., Vol. 43 (1981), No. 334, pp. 21–54.

[9] K. Nanbu, Slowing Down of Energetic Molecules in a Spatially Uniform Gas, Rep. Inst. High Speed Mech., Tōhoku Univ., Vol. 43 (1981), No. 335, pp. 55–88.

[10] K. Nanbu, Direct Simulation Scheme Derived from the Boltzmann Equation. IV. Correlation of Velocity, J. Phys. Soc. Japan, Vol. 50 (1981), pp. 2829–2836.

[11] K. Nanbu: Direct Simulation Scheme Derived from the Boltzmann Equation. V. Effects of Sample Size, Number of Molecules, Step Size, and Cut-Off Angle upon Simulation Data, Rep. Inst. High Speed Mech., Tōhoku Univ., Vol. 45 (1982), No. 348, pp. 19–41.

[12] K. Nanbu: Exact Direct-Simulation-Scheme for the Boltzmann Equation/Correlation of Molecular Velocities Subject to Renewal Processes, Proceedings of the Symposium on Mechanics for Space Flight, Report S. P. 1, pp. 109–22. (Inst. Space Aero. Sci., 1982).

[13] Y. Watanabe and K. Nanbu: Direct Simulation Scheme Derived from the Boltzmann Equation. VII. Ergodicity of Simulation Solutions, Rep. Inst. High Speed Mech., Tōhoku Univ., Vol. 45 (1982), No. 349, pp. 43–76.

[14] C-Y. Liu and L. Lees: Kinetic Theory Description of Plane Compressible Couette Flow, *Rarefied Gas Dynamics* (Advances in Applied Mechanics, Supplement 1), ed. L. Talbot, Academic Press, New York, 1961, pp. 391–428.

[15] Handbook of Mechanical Engineering (Japan Soc. Mech. Engineers, Tōkyo, 1968), 5th ed., Chap. 2, p.3 (in Japanese).

[16] S. A. Schaaf and P. L. Chambré: Flow of Rarefied Gases, in *Fundamentals of Gas Dynamics* (High Speed Aerodynamics and Jet Propulsion, Vol. III), ed. H. W. Emmons, Princeton Univ. Press, Princeton, 1958, p. 709.

[17] P. A. Lagerstrom: Laminar Flow Theory, in *Theory of Laminar Flows* (High Speed Aerodynamics and Jet Propulsion, Vol. IV), ed. F. K. Moore, Princeton Univ. Press, Princeton, pp. 171–175.

[18] S. A. Schaaf and P. L. Chambré: Flow of Rarefied Gases, in *Fundamentals of Gas Dynamics* (High Speed Aerodynamics and Jet Propulsion, Vol. III), ed. H. W. Emmons, Princeton Univ. Press, Princeton, 1958, pp. 718–719.